Journal of Engineering Mathematics, Vol. 6, No. 2, April 1972
Wolters-Noordhoff Publishing–Groningen
Printed in the Netherlands

Some Cases of Interface Flow Towards Drains

O. D. L. STRACK

Laboratory of Soil Mechanics, Delft University of Technology, The Netherlands

(Received July 30, 1971)

SUMMARY
The aim of the study, reported of in this paper, is to determine the shape and position of the interface which separates the fresh from the salt water in a coastal aquifer. In this aquifer, fresh water flows from land towards the sea because the head on the land is higher than on the seabottom. The upper boundary of the flow region, formed by the land surface and the seabottom has been approximated by a straight line.

Firstly the problem is solved, by use of the method of conformal mapping and the hodograph, for the case that the head is constant along that part of the line which represents the land surface and also constant, but lower, on the part which represents the seabottom. Special attention is paid to the form and position of the interface when a drain is in operation in the fresh water region.

The hodograph turns out to be multiple sheeted and contains internal branch points and poles. Therefore, a simple generalization of the Schwarz–Christoffel Integral is derived which maps such hodographs onto the upper half plane.

Secondly it is shown that the solution can be generalized directly by superposition in the reference half plane. This permits the description of the flow case of an arbitrary number of drains. By superposition, also flow with drains and an arbitrary number of different levels in polders and dunes can be described.

Thirdly the upconing of the interface under a drain is studied in more detail for a simple case.

A test was run in a parallel plate model in order to verify some of the formulas for upcoming, derived in this paper. Test results and theory agree satisfactorily.

1. Introduction

In coastal aquifers there often exists a situation in which the interface between fresh and salt water is steady. In most cases the flow rates in the salt water region are much lower than those in the fresh and may therefore be neglected. It is of practical interest to know the position and shape of the interface under various conditions. This is the case, for instance, when the interface cones up under a drain and when in a polder a relatively low head is maintained so that the interface rises. In the first case, brackish water will appear in the drain if the upconing is too large and in the second case the rising of the interface can be harmful for the vegetation in the polder.

The mathematical description of the real situation is rather complicated and therefore some simplifications will be made. It is supposed that the fresh and salt water are divided by an interface rather than a transition zone, and that the salt water is at rest. Inhomogenities of the permeability are neglected, and only two-dimensional flow problems will be considered.

As an example of the flow problems that can be treated with the methods developed in this paper, consider the flow of fresh water above salt water at rest in a coastal aquifer (see Fig. 1).

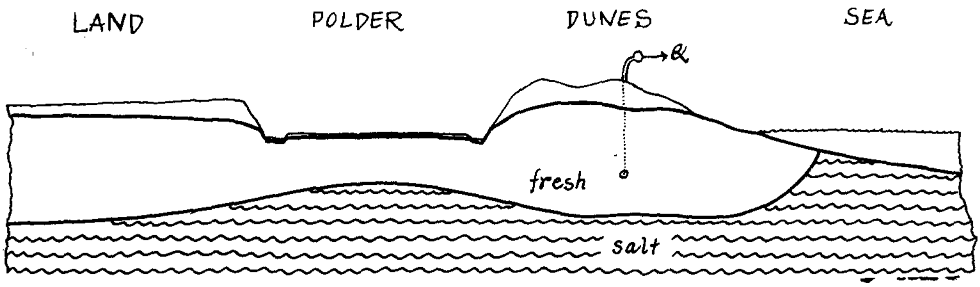

Figure 1. The coastal aquifer.

In the dune area a relatively high head is maintained, while in a polder more land inwards, the head is lower. On the land side the polder is bounded by a region where the head is maintained on a level, higher than on the seabottom. Due to the differences in the head, flow will occur in the fresh water zone. One or more drains may be in operation somewhere in the flow region.

Even with the simplifications mentioned above, the exact solutions of such flow problems are rather complicated and consequently not very useful for practice. Therefore, some further approximations will be made in the subsequent study.

The influence of drains on the shape of the interface in coastal aquifers has been investigated by various authors [1], [2], [3]. In these investigations, the upper boundary of the flow region is usually approximated by an impervious layer. This leads to a flow case which describes correctly the situation close to the coast. However, a disadvantage of this flow case is that all of the fresh water is coming from infinity which causes a continued lowering of the interface towards infinity. In this paper the more realistic case will be considered that fresh water is supplied from above (for instance infiltration water, supplied by canals, lakes, etc.). This is done by approximating the upper boundary of the flow region by straight lines of constant head. (see Fig. 2.)

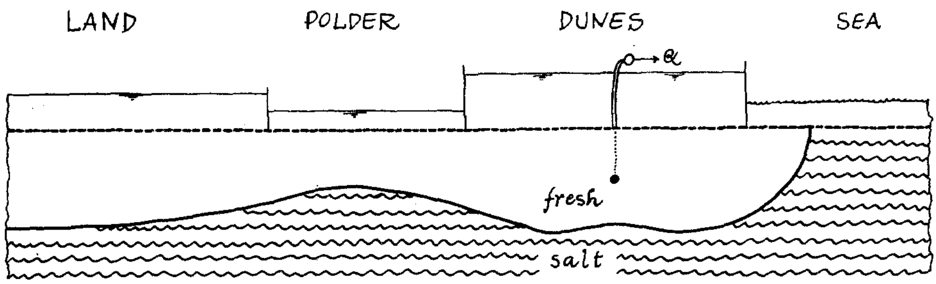

Figure 2. The flow case, which approximates the coastal aquifer of Fig. 1. (The dashed line is the soil surface).

The flow problem which is obtained in this way can be solved analytically by means of the method of conformal mapping. The form of the solution will be given for the general flow case. In that case an arbitrary number of polders are present in addition to the dunes, as well as strips of land where a higher head is maintained. An arbitrary number of drains or negative drains are in operation somewhere in the flow region.

In the literature on groundwater flow, problems of this kind are solved by use of hodographs. No solutions are known for interface problems where an arbitrary number of drains or negative drains are located arbitrarily inside the flow region. A difficulty in such problems is, that the hodograph, although an elegant tool, becomes multiple sheeted and may contain internal branch points of which the position depends on the solution. Furthermore, the complex potential function is double valued along the dividing streamlines. De Josselin de Jong [2] was the first to solve an interface problem with a double sheeted hodograph with a sink, located on the boundary. The branch points of the hodograph were restricted to lie on the boundary also.

It will be shown in this paper that multiple sheeted hodographs with sinks (i.e. poles) and branch points which are not located on the boundary can be mapped onto the upper half plane by a simple generalization of the Schwarz–Christoffel Integral. Moreover, the complication of the double valuedness of the complex potential along the dividing streamlines will be eliminated.

Furthermore it shall be shown that the solution for the flow case with dunes and an arbitrary number of polders and of drains in operation can be derived directly from the solution with one drain and dunes only. It appears that the parametric form of the latter solution permits superposition in the reference plane.

In section 5, the upconing of the interface under a drain, which can lead to brackish water in

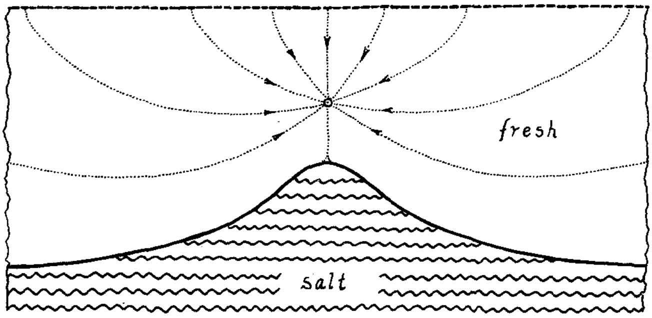

Figure 3. Upconing under a drain.

the drainpipe, will be studied in more detail. To this end, the foregoing flow case is simplified by leaving out the sea as well as the differences in the head on the land surface (see Fig. 3). Finally, in section 6, a report is made of some tests, carried out to verify some of the formulas for upconing, derived in this paper.

2. The Map of the Interface onto the Hodograph Plane

It follows from Darcy's law: [5], [6]

$$\boldsymbol{q} = -k \operatorname{grad} \phi = -\operatorname{grad} \Phi \tag{2.1}$$

(where $\boldsymbol{q}=(q_x, q_y)$ is the specific discharge vector, k the coefficient of permeability and ϕ the head), and from the continuity equation:

$$\operatorname{div}(\boldsymbol{q}) = 0 \tag{2.2}$$

that Φ, the velocity potential, must be a harmonic function of x and y (x and y are the rectangular coordinates in the physical plane). A function $\Psi(x, y)$, also harmonic, can be found, such that the complex potential:

$$\Omega = \Phi + i\Psi \tag{2.3}$$

is an analytic function of $z = x+iy$. Then, the method of conformal mapping can be used in order to determine $\Omega = \Omega(z)$.

The hodograph $(q_x + iq_y)$ is related to Ω as follows:

$$q_x + iq_y \doteq -\frac{d\bar{\Omega}}{d\bar{z}} = -\bar{w}$$

where the bar indicates the complex conjugate. The analytic function

$$w = -\frac{d\Omega}{dz} \tag{2.4}$$

is the complex conjugate of the hodograph and is known as the specific discharge function.

For the solution of interface problems, the hodograph can be used in order to avoid the complication that the interface is unknown. In the hodograph plane the interface is a circle [5], [6] as can be shown as follows. To start with, it is remarked that the equilibrium of the interface requires that the pressures in the fresh and salt water are equal in any point of the interface (see Fig. 4). Furthermore, the salt water is assumed to be at rest and therefore the pressure varies hydrostatically there:

$$p_f = p_s = a - \gamma_s \cdot y \tag{2.5}$$

where p_s and p_f are the pressures in the salt and fresh water and a represents a constant. The specific weights of fresh and salt water are respectively γ_s and γ_f. Eq. (2.5) enables one to express the fresh water head (ϕ) as a function of y, because the salt water is at rest so that the head is

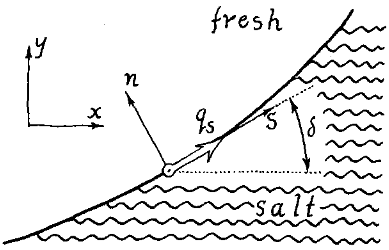

Figure 4. Detail of the interface.

constant there. Hence:

$$\phi = \Phi/k = y + p_f/\gamma_f = a/\gamma_f - y\cdot(\gamma_s - \gamma_f)/\gamma_f\,. \tag{2.6}$$

Now, the specific discharge along the interface can be derived from eqs. (2.1) and (2.6). This gives:

$$\begin{aligned} q_s &= -k(\partial\phi/\partial s) = -\partial\Phi/\partial s \\ &= k[(\gamma_s - \gamma_f)/\gamma_f](\partial y/\partial s) \\ &= k^*(\partial y/\partial s) = k^* \sin(\delta) \end{aligned}$$

where δ is the inclination of the interface (see Fig. 4), and where:

$$k^* = [(\gamma_s - \gamma_f)/\gamma_f]\cdot k\,. \tag{2.7}$$

Furthermore, the interface is a streamline and the component of the specific discharge vector normal to the interface must be zero.

Hence:

$$q_x^2 + q_y^2 = (k^*)^2 \sin^2(\delta)$$
$$q_y/q_x = \tan(\delta)\,.$$

Elimination of δ from these two equations gives:

$$q_x^2 + q_y^2 - k^* q_y = 0 \tag{2.8}$$

which in the hodograph plane represents a circle, passing through the origin and with radius $\frac{1}{2}k^*$.

3. Interface Flow with One Drain and One Discontinuity in the Head.

3.1. *The Hodograph*

Firstly, the hodograph will be investigated for the flow problem without a drain*. Then, on the land surface which extends from the coast (C, see Fig. 5a) to A_2 (infinity) the head is maintained on a constant level. The head on the seabottom which extends from the coast (C) over B to infinity (see Fig. 5a), is also constant. Since the head on the seabottom is lower than on land, fresh water flows from land to sea above salt water at rest. This salt water is pressed down by the fresh and extends under land.

The hodograph for this flow problem will be constructed now. As is explained in the preceding section, the interface is mapped onto a circle in the hodograph plane (AB, see Fig. 5b). At A (infinity), the specific discharge is zero, because the influence of the difference in the head on land and seabottom vanishes at infinity. The specific discharge vector is directed vertically upwards at B, because BC is a line of constant head. For the same reason the specific discharge vector is directed vertically upwards along BC. At C, the absolute value of the specific discharge vector is unlimited since C is a corner point. On the land surface (CA_2) the head is constant and the specific discharge vector points vertically downwards.

* This flow problem has been solved by Polubarinova-Kochina [7], pp. 355–356.

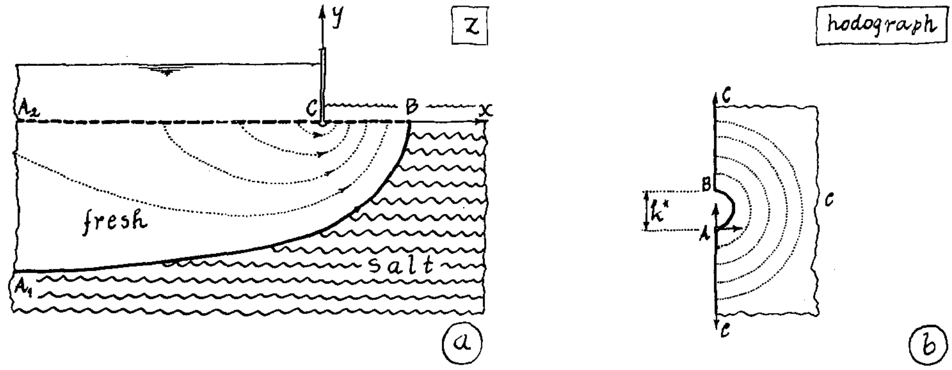

Figure 5. Interface flow from land to sea.

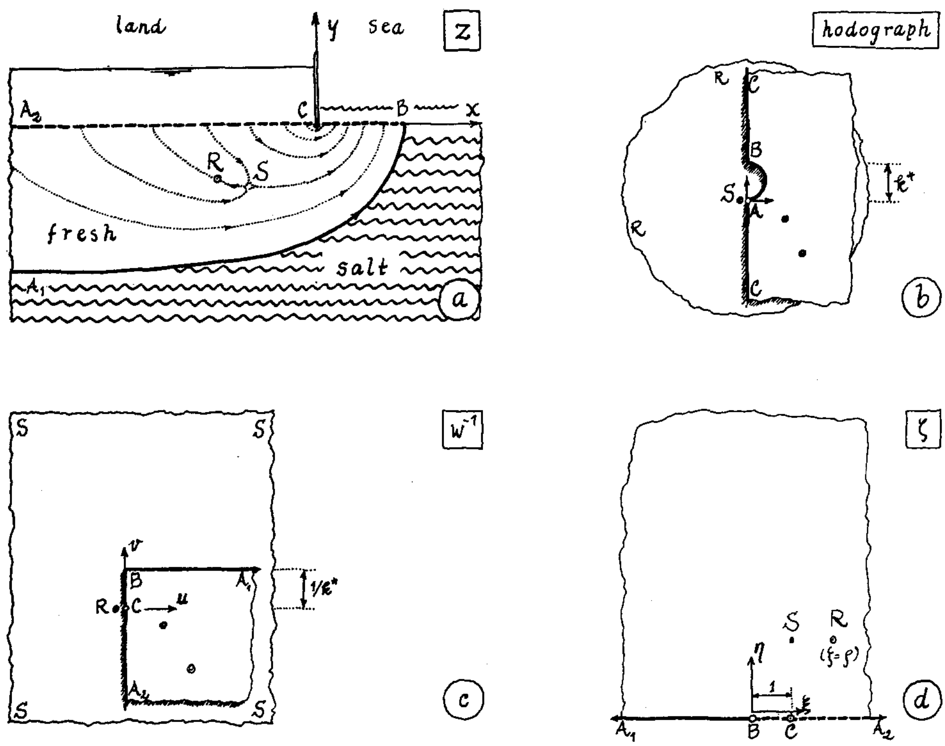

Figure 6. Fresh water flows from land partly towards the sea and partly to the drain.

Secondly the hodograph will be investigated for the flow where a drain (R, see Fig. 6a) is in operation somewhere in the flow region. At this drain, the specific discharge vector is inifinite because the drain is schematized to a point. So, there are two points where the specific discharge vector is infinite (C and R). Furthermore, a stagnation point (S, Fig. 6a) will appear in the flow region so that there is a zero-discharge at two points (A and S). Since an infinite specific discharge corresponds to two different points in z (C and R) as well as a zero-discharge to two other different points in z (A and S), the hodograph consists of two sheets (see Fig. 6b). The shape of the first sheet, ABC, is unchanged, if compared with the flow without the drain (see Fig. 5b). The second sheet contains the images of the drain and the stagnation point. As can be deduced from the results, obtained in the appendix, the two sheets in this case are connected by two internal branch points.

In order to facilitate the procedure of conformal mapping, which will be carried out later, the specific discharge function ($w = q_x - iq_y$) is inverted. Then the region in the w^{-1}-plane ($w^{-1} = (q_x - iq_y)^{-1} = u + iv$) of Fig. 6c is obtained, which is bounded by straight line segments, because the circular arc (BA, see Fig. 6b) is transformed to the straight line $v=i/k^*$ (BA_1, see Fig. 6c).

Now that the region in the w^{-1}-plane is known, the flow problem can be solved by means of the method of conformal mapping. This will be done in the following way. Firstly the region (ABCSR) in the w^{-1}-plane of Fig. 6c will be mapped onto the reference half plane im $\zeta \geq 0$ of Fig. 6d. Secondly, (in the next section) the complex potential, Ω, will be determined as a function of the same reference parameter (ζ). Then, by use of the relation (2.4) between Ω, w^{-1} and z, the latter can be found as a function of ζ:

$$z = -\int w^{-1}(\zeta)\,[d\Omega(\zeta)/d\zeta]\,d\zeta + C\,. \tag{3.1}$$

Finally, the solution is given by $\Omega=\Omega(\zeta)$ and $z=z(\zeta)$ which are known functions of the same reference parameter, ζ.

The region in the w^{-1}-plane of Fig. 6c will be mapped conformally onto the reference plane of Fig. 6d now. As is shown in the appendix, the mapping function is of the following form:

$$w^{-1} = \alpha \int_0^{\zeta} \lambda^{-\frac{1}{2}} \prod_{i=1}^{2} \{(\lambda-\gamma_i)(\lambda-\bar{\gamma}_i)\}\,[(\lambda-\sigma)(\lambda-\bar{\sigma})]^{-2}\,d\lambda + \beta\,, \tag{3.2}$$

where σ denotes the position of the stagnation point in ζ, and where γ_i denote the branch points. Point A is mapped onto infinity, point B onto $\zeta=0$, and point C onto $\zeta=1$ (see Fig. 6d). Because w^{-1} equals i/k^* at point B (see Fig. 6c), $\beta=i/k^*$.

Integration of eq. (3.2) gives:

$$w^{-1} = \frac{i}{k^*} + A\,\frac{(\zeta-p)(\zeta-\bar{p})}{(\zeta-\sigma)(\zeta-\bar{\sigma})}\cdot \zeta^{\frac{1}{2}} \tag{3.3}$$

where the condition is used, that:

$$\operatorname*{Res}_{\zeta=\sigma}\,[dw^{-1}/d\zeta] = 0$$

(see the appendix, eq. (A.4)), and where A and p can be expressed in σ and k^*.

3.2. *The Complex Potential*

The complex potential (Ω) as a function of the reference parameter will be derived by solving the flow problem in the reference plane. Consider the complex potential $\Omega^*=\Phi^*+i\Psi^*$ for the flow in im $\zeta \geq 0$ which originates if A_1B (see Fig. 7a) is a streamline and along BC the value for Φ^* is zero and along CA_2 it is kH. A drain is located in $\zeta=\rho$. Since (by Riemann's Theorem) the ζ-plane can be considered as the conformal map of the physical plane, it follows that $\Omega^*(\zeta)$ must equal $\Omega(\zeta)$, the function in search.

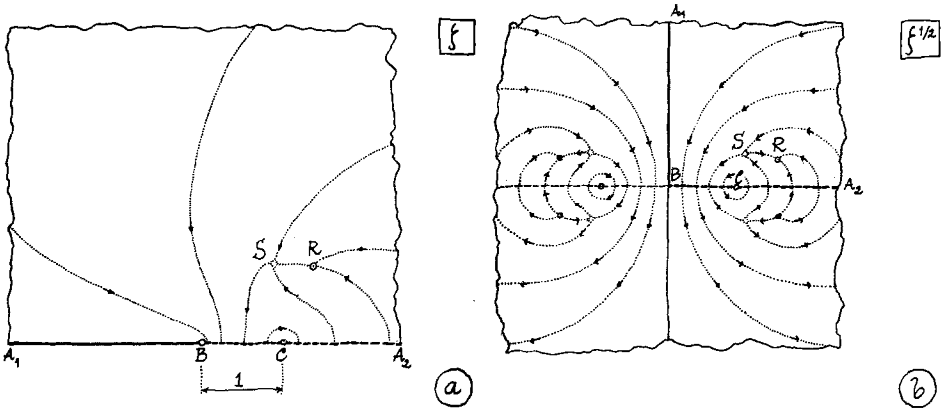

Figure 7. The fictitious flow in the reference plane.

$\Omega=\Omega(\zeta)$ is the solution for the flow in ζ of which a sketch is given in Fig. 7a. This flow problem can be solved easier if the ζ half plane is transformed into a quarter plane ($\zeta^{\frac{1}{2}}$). The $\zeta^{\frac{1}{2}}$-plane is drawn in Fig. 7b. The reference plane (im $\zeta \geqq 0$, Fig. 7a) is mapped onto the upper right quadrant (see Fig. 7b). Since A_1B is a streamline and BC and CA_2 are lines of constant head, the flow in the $\zeta^{\frac{1}{2}}$-plane must be symmetric with respect to A_1B and antisymmetric with respect to BCA_2. Hence, if a drain operates at $\zeta^{\frac{1}{2}}=\rho^{\frac{1}{2}}$, a drain must be introduced at $\zeta^{\frac{1}{2}}=-\bar{\rho}^{\frac{1}{2}}$ and negative drains at $\zeta^{\frac{1}{2}}=-\rho^{\frac{1}{2}}$ and at $\zeta^{\frac{1}{2}}=\bar{\rho}^{\frac{1}{2}}$. Furthermore, along A_2C the value of Φ is kH and along CB it is zero. The elementary solution, describing the flow round a vortex with strength kH in C ($\zeta^{\frac{1}{2}}=1$) satisfies these conditions. A countervortex with strength $-kH$ must be introduced at $\zeta^{\frac{1}{2}}=-1$, in order that the flow in $\zeta^{\frac{1}{2}}$ (see Fig. 7b) is symmetric with respect to A_1B and antisymmetric with respect to BCA_2. Hence, the solution is of the following form:

$$\Omega=\frac{kH}{\pi}\,i\ln\frac{\zeta^{\frac{1}{2}}-1}{\zeta^{\frac{1}{2}}+1}+\frac{Q}{2\pi}\ln\frac{(\zeta^{\frac{1}{2}}-\rho^{\frac{1}{2}})(\zeta^{\frac{1}{2}}+\bar{\rho}^{\frac{1}{2}})}{(\zeta^{\frac{1}{2}}-\bar{\rho}^{\frac{1}{2}})(\zeta^{\frac{1}{2}}+\rho^{\frac{1}{2}})}+kH\,, \tag{3.4}$$

One finds z as a function of ζ by integration of eq. (3.1). The first term of the integrand of this equation, $w^{-1}(\zeta)$, has already been determined (see eq. (3.3)). The second term, $d\Omega(\zeta)/d\zeta$ can be obtained from eq. (3.4) by differentiation. This gives:

$$\frac{d\Omega(\zeta)}{d\zeta}=\frac{kHi(\zeta-\rho)(\zeta-\bar{\rho})+\frac{1}{2}Q(\zeta-1)(\zeta+\rho\bar{\rho})(\rho^{\frac{1}{2}}-\bar{\rho}^{\frac{1}{2}})}{\pi(\zeta-1)(\zeta-\rho)(\zeta-\bar{\rho})\zeta^{\frac{1}{2}}}\,. \tag{3.5}$$

The specific discharge is zero at the stagnation point, and the map of z onto im $\zeta \geqq 0$ must be conformal there. Therefore, it follows from eq. (2.4):

$$w=-\frac{d\Omega(\zeta)}{d\zeta}\cdot\frac{d\zeta}{dz}\,,$$

that $d\Omega(\zeta)/d\zeta$ must be zero at the stagnation point, so that $\zeta=\sigma$ is a root of the numerator of eq. (3.5). Furthermore, if the numerator is divided by i, the remaining expression is symmetric with respect to the real axis. Hence, $\zeta=\bar{\sigma}$ is also a root of this numerator and therefore, eq. (3.5) can be written in the following form:

$$\frac{d\Omega(\zeta)}{d\zeta}=B\cdot\frac{(\zeta-\sigma)(\zeta-\bar{\sigma})}{(\zeta-\rho)(\zeta-\bar{\rho})}\cdot\frac{1}{(\zeta-1)\zeta^{\frac{1}{2}}}\,, \tag{3.6}$$

where B is a constant. z can be found as a function of ζ by use of eqs. (3.1), (3.3),), (3.4), and (3.6). This yields:

$$z=\frac{kH}{\pi k^*}\ln\frac{\zeta^{\frac{1}{2}}-1}{\zeta^{\frac{1}{2}}+1}-\frac{Q}{2\pi k^*}\,i\ln\frac{(\zeta^{\frac{1}{2}}-\rho^{\frac{1}{2}})(\zeta^{\frac{1}{2}}+\bar{\rho}^{\frac{1}{2}})}{(\zeta^{\frac{1}{2}}-\bar{\rho}^{\frac{1}{2}})(\zeta^{\frac{1}{2}}+\rho^{\frac{1}{2}})}-\mathrm{AB}\int\frac{(\zeta-p)(\zeta-\bar{p})}{(\zeta-1)(\zeta-\rho)(\zeta-\bar{\rho})}\,d\zeta+\mathrm{D}$$

Evaluation of the integral gives, taking into account that z is zero in C ($\zeta=1$) and finite at the drain as well as $y=0$ along A_2CB:

$$z=-2\frac{kH}{\pi k^*}\ln\left[\tfrac{1}{2}(\zeta^{\frac{1}{2}}+1)\right]+\frac{Q}{\pi k^*}\,i\ln\frac{\zeta^{\frac{1}{2}}+\rho^{\frac{1}{2}}}{\zeta^{\frac{1}{2}}+\bar{\rho}^{\frac{1}{2}}}+\frac{2Q}{\pi k^*}\arg(1+\rho^{\frac{1}{2}})\,. \tag{3.7}$$

Separation of eq. (3.7) into real and imaginary parts gives:

$$x=-\frac{kH}{\pi k^*}\ln\tfrac{1}{4}(\lambda+2\lambda^{\frac{1}{2}}\cos\tfrac{1}{2}\theta+1)-\frac{Q}{\pi k^*}\arctan\left\{\frac{2r^{\frac{1}{2}}\sin\frac{1}{2}\alpha\left[\lambda^{\frac{1}{2}}\cos\frac{1}{2}\theta+r^{\frac{1}{2}}\cos\frac{1}{2}\alpha\right]}{\lambda+2(\lambda r)^{\frac{1}{2}}\cos\frac{1}{2}\theta\cos\frac{1}{2}\alpha+r\cos\alpha}\right\}$$
$$+\frac{2Q}{\pi k^*}\arctan\left[\frac{r^{\frac{1}{2}}\sin\frac{1}{2}\alpha}{1+r^{\frac{1}{2}}\cos\frac{1}{2}\alpha}\right] \tag{3.8}$$

$$y=-\frac{2kH}{\pi k^*}\arctan\left[\frac{\lambda^{\frac{1}{2}}\sin\frac{1}{2}\theta}{1+\lambda^{\frac{1}{2}}\cos\frac{1}{2}\theta}\right]+\frac{Q}{2\pi k^*}\ln\left[\frac{\lambda+2(\lambda r)^{\frac{1}{2}}\cos\frac{1}{2}(\alpha-\theta)+r}{\lambda+2(\lambda r)^{\frac{1}{2}}\cos\frac{1}{2}(\alpha+\theta)+r}\right] \tag{3.9}$$

where:

$$\zeta = \lambda\, e^{i\theta}$$

and:

$$\rho = r\, e^{i\alpha}.$$

The position of the drain in z ($z_R = x_R + iy_R$) can be related to its position in ζ ($\rho = r\,e^{i\alpha}$) by putting $\lambda = r$, $\theta = \alpha$ in eqs. (3.8) and (3.9). This yields:

$$x_R = -\frac{kH}{\pi k^*} \ln \tfrac{1}{4}(r + 2r^{\frac{1}{2}} \cos \tfrac{1}{2}\alpha + 1) - \frac{Q}{\pi k^*} \cdot \tfrac{1}{2}\alpha + \frac{2Q}{\pi k^*} \arctan \left[\frac{r^{\frac{1}{2}} \sin \frac{1}{2}\alpha}{1 + r^{\frac{1}{2}} \cos \frac{1}{2}\alpha}\right] \tag{3.10}$$

$$y_R = -\frac{2kH}{\pi k^*} \arctan \left[\frac{r^{\frac{1}{2}} \sin \frac{1}{2}\alpha}{1 + r^{\frac{1}{2}} \cos \frac{1}{2}\alpha}\right] - \frac{Q}{\pi k^*} \ln (\cos \tfrac{1}{2}\alpha). \tag{3.11}$$

The relations (3.10) and (3.11) can only be given in parametric form so that if x_R and y_R are given, r and α must be computed numerically.

The equation for the interface in the physical plane can be found in parametric form from eqs. (3.8) and (3.9) by putting $\theta = \pi$ (the interface is mapped onto the negative ξ-axis, cf. Fig. 6). This yields:

$$x = -\frac{kH}{\pi k^*} \ln \tfrac{1}{4}(\lambda + 1) - \frac{Q}{\pi k^*} \arctan \left[\frac{r \sin \alpha}{\lambda + r \cos \alpha}\right] + \frac{2Q}{\pi k^*} \arctan \left[\frac{r^{\frac{1}{2}} \sin \frac{1}{2}\alpha}{1 + r^{\frac{1}{2}} \cos \frac{1}{2}\alpha}\right] \tag{3.12}$$

$$y = -\frac{2kH}{\pi k^*} \arctan \lambda + \frac{Q}{2\pi k^*} \ln \left[\frac{\lambda + 2(\lambda r)^{\frac{1}{2}} \sin \frac{1}{2}\alpha + r}{\lambda - 2(\lambda r)^{\frac{1}{2}} \sin \frac{1}{2}\alpha + r}\right]. \tag{3.13}$$

Finally the position of point B, which lies on the interface and which is mapped onto $\zeta = 0$, (cf. Fig. 6) can be found from eq. (3.12) by putting $\lambda = 0$. This gives:

$$x_B = \frac{kH}{\pi k^*} \ln 4 - \frac{Q}{\pi k^*} \alpha + \frac{2Q}{\pi k^*} \arctan \left[\frac{r^{\frac{1}{2}} \sin \frac{1}{2}\alpha}{1 + r^{\frac{1}{2}} \cos \frac{1}{2}\alpha}\right]. \tag{3.14}$$

4. Flow with an Arbitrary Number of Drains and an Arbitrary Number of Discontinuities of Φ on the Land Surface

The solution of the groundwater flow problem, treated in the preceding section, is given in parametric form. The parameter, ζ, cannot be eliminated, except in case the discharge of the drain is zero. Therefore, the position of the drain in the reference plane must be known. It can be found from given data in the physical plane, but only by means of numerical methods. However, a considerable benefit of the parametric form is that the solution which describes the flow with an arbitrary number of drains and of discontinuities in Φ on the land surface can be found simply by superposition. This will be shown now.

To start with, the solution for flow with one discontinuity in Φ and one drain will be studied again. This solution has been given in the preceding section in the form of the following two equations (see eqs. (3.4) and (3.7)):

$$\Omega = \frac{kH}{\pi} i \ln \frac{(\zeta^{\frac{1}{2}} - 1)}{(\zeta^{\frac{1}{2}} + 1)} + \frac{Q}{2\pi} \ln \frac{(\zeta^{\frac{1}{2}} - \rho^{\frac{1}{2}})(\zeta^{\frac{1}{2}} + \bar{\rho}^{\frac{1}{2}})}{(\zeta^{\frac{1}{2}} - \bar{\rho}^{\frac{1}{2}})(\zeta^{\frac{1}{2}} + \rho^{\frac{1}{2}})} + kH \tag{4.1}$$

$$z = -\frac{2kH}{\pi k^*} \ln \tfrac{1}{2}(\zeta^{\frac{1}{2}} + 1) + \frac{Q}{\pi k^*} i \ln \frac{(\zeta^{\frac{1}{2}} + \rho^{\frac{1}{2}})}{(\zeta^{\frac{1}{2}} + \bar{\rho}^{\frac{1}{2}})} + \frac{2Q}{\pi k^*} \arg (1 + \rho^{\frac{1}{2}}). \tag{4.2}$$

One may write these two equations in the following symbolic form:

$$\Omega = \Omega_v(\zeta, 1) + \Omega_d(\zeta, \rho) + C_1 \tag{4.3}$$

$$z = z_v(\zeta, 1) + z_d(\zeta, \rho) + C_2 \tag{4.4}$$

where:

$$\Omega_v(\zeta, \nu) = \frac{kH}{\pi} i \ln \frac{(\zeta^{\frac{1}{2}} - \nu^{\frac{1}{2}})}{(\zeta^{\frac{1}{2}} + \nu^{\frac{1}{2}})} \tag{4.5}$$

$$z_v(\zeta, \nu) = -\frac{2kH}{\pi k^*} \ln \tfrac{1}{2}(\zeta^{\frac{1}{2}} + \nu^{\frac{1}{2}}) \tag{4.6}$$

and where $\Omega_d(\zeta, \rho)$ and $z_d(\zeta, \rho)$ represent the second terms of eqs. (4.1) and (4.2) respectively. The solution, represented by eqs. (4.3) and (4.4) has been constructed in such a way that it satisfies all boundary conditions, including the condition along the interface which may be characterised by the following equation (cf. eq. (2.6)):

$$\Phi = -k^* \cdot y\,. \tag{4.7}$$

Furthermore, eqs. (4.3) and (4.4) are valid for all complex ρ. Now, consider the following functions:

$$\Omega = \sum_{\mu=1}^{m} \Omega_v(\zeta, \nu_\mu) + \sum_{j=1}^{n} \Omega_d(\zeta, \rho_j) + C_1 \tag{4.8}$$

$$z = \sum_{\mu=1}^{m} z_v(\zeta, \nu_\mu) + \sum_{j=1}^{n} z_d(\zeta, \rho_j) + C_2 \tag{4.9}$$

where m is the number of vortices at $\zeta = \nu_\mu$ ($\mu = 1, 2, 3, \ldots, m$), and n the number of drains or negative drains at $\zeta = \rho_j$ ($j = 1, 2, 3, \ldots, n$). It can be verified, that these functions satisfy the condition along the interface (4.7) as well as all other boundary conditions. Therefore, eqs. (4.8) and (4.9) together represent the solution.

Substitution of the functions, given in eqs. (4.1), (4.2), (4.5) and (4.6) for Ω_v, Ω_d, z_v and z_d in eqs. (4.8) and (4.9) yields:

$$\Omega = \sum_{\mu=1}^{m} \frac{k(\Delta H_\mu)}{\pi} i \ln \frac{(\zeta^{\frac{1}{2}} - \nu_\mu^{\frac{1}{2}})}{(\zeta^{\frac{1}{2}} + \nu_\mu^{\frac{1}{2}})} + \sum_{j=1}^{n} \frac{Q_j}{2\pi} \ln \frac{(\zeta^{\frac{1}{2}} - \rho_j^{\frac{1}{2}})(\zeta^{\frac{1}{2}} + \bar{\rho}_j^{\frac{1}{2}})}{(\zeta^{\frac{1}{2}} - \bar{\rho}_j^{\frac{1}{2}})(\zeta^{\frac{1}{2}} + \rho_j^{\frac{1}{2}})} + C_1 \tag{4.10}$$

$$z = -2 \sum_{\mu=1}^{m} \frac{k(\Delta H_\mu)}{\pi k^*} \ln \tfrac{1}{2}(\zeta^{\frac{1}{2}} + \nu_\mu^{\frac{1}{2}}) + \sum_{j=1}^{n} \frac{Q_j}{\pi k^*} i \ln \frac{(\zeta^{\frac{1}{2}} + \rho_j^{\frac{1}{2}})}{(\zeta^{\frac{1}{2}} + \bar{\rho}_j^{\frac{1}{2}})} + C_2\,. \tag{4.11}$$

In these equations, (ΔH_μ) is the amount by which the head increases if the μ^{th} vortex is passed in z, going from the right to the left (see Fig. 8).

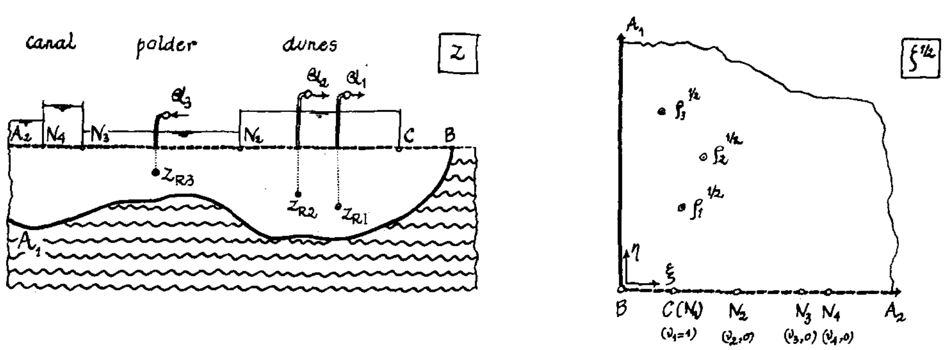

Figure 8. The generalization of the flow problem.

The constants C_1 and C_2 can be found in the same way as is done in section 3. The parameters $\nu_1, \nu_2, \ldots, \nu_m$ ($\nu_1 = 1$) and $\rho_1, \rho_2, \ldots, \rho_n$ can be determined numerically from given data in the physical plane as follows. In each vortex the value of z is known ($z = x_{N_i}$) as well as in each drain ($z = x_{R_j} + iy_{R_j}$). Substitution of the values for ζ which correspond to these points ($\zeta = \nu_1, \ldots, \nu_m$ and $\zeta = \rho_1, \ldots, \rho_n$ respectively) in eqs. (4.10) and (4.11) leads to m real and n complex equations, which are sufficient for the determination of the m real parameters ν_i and the n complex parameters ρ_j.

5. Upconing

When for water supply a drain above an interface is used, upconing occurs which may lead to the presence of brackish water in the drainpipe. This causes a considerable lowering of the water quality. Because there are reasons to suspect that the magnitude of the upconing is related to the amount of brackish water in the drainpipe, it is of interest to relate the upconing to the position and the discharge of the drain. Furthermore, one must know the maximal discharge of the drain for which the interface just remains stable (see Fig. 9b). This discharge depends on the position of the drain (cf. [1]). The upconing is pictured in Fig. 9a.

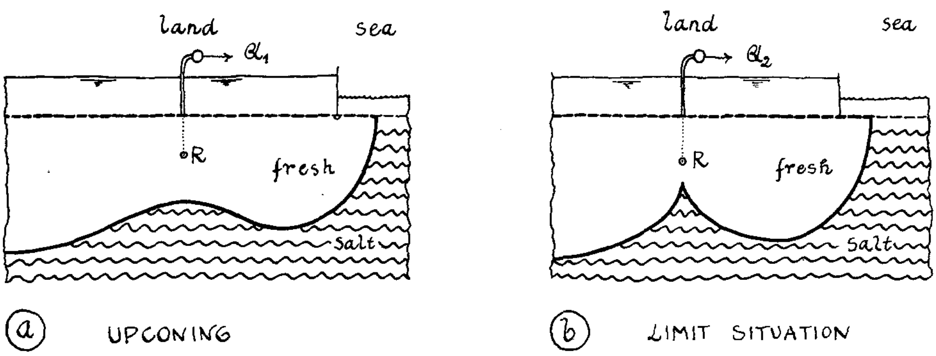

Figure 9. Upconing in the coastal aquifer.

In order to reduce the number of the parameters involved, the flow case will be studied where the influence of the seabottom is not taken into consideration and where there are no differences in the head on the land surface (see Fig. 10a). Now, no fresh water flows to the seabottom and C and B form one point in z (infinity, see Fig. 10a). The coordinate system in $z(x, y)$ is chosen as follows. The y-axis points vertically upwards and passes through the drain (R, see Fig. 10a). The x-axis is chosen along the interface in the position when no fresh water is extracted by the drain. S (the stagnation point) and D are the intersection points of the y-axis with the interface (A_1SB) and the line of constant head (CDA_2) respectively (see Fig. 10a). The distance between the x-axis and CDA_2 is H. Furthermore, the value of Φ along CDA_2 is now chosen to be zero:

$$\Phi_{CDA_2} = 0 \,. \tag{5.1}$$

The ζ-plane is characterized by the following points. B and C are mapped onto $\zeta = 0$; S onto $\zeta = -1$ and A onto $\zeta = \infty$ (see Fig. 10b). Because the region in z (see Fig. 10a) is symmetric with

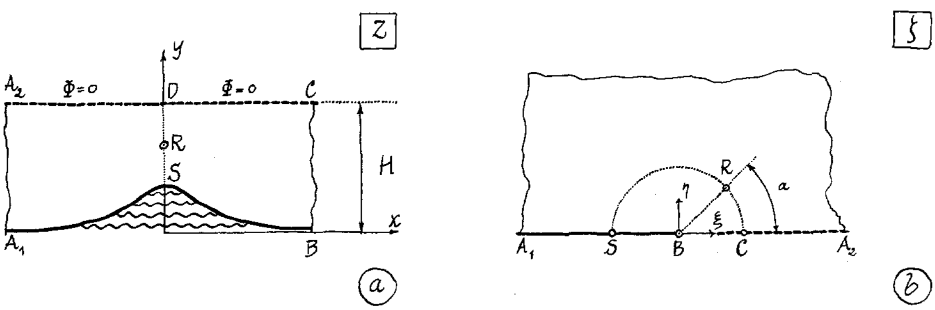

Figure 10. Upconing.

respect to the line DRS, this line will be mapped onto the unit circle in ζ (see Fig. 10a). It can be verified, that eqs. (3.4) and (3.7) now reduce to:

$$\Omega = \frac{Q}{2\pi} \ln \frac{(\zeta^{\frac{1}{2}}-\rho^{\frac{1}{2}})(\zeta^{\frac{1}{2}}+\bar{\rho}^{\frac{1}{2}})}{(\zeta^{\frac{1}{2}}-\bar{\rho}^{\frac{1}{2}})(\zeta^{\frac{1}{2}}+\rho^{\frac{1}{2}})} \tag{5.2}$$

$$z = -\frac{H}{\pi} \ln \zeta + \frac{Q}{\pi k^*} i \ln \frac{\zeta^{\frac{1}{2}}+\rho^{\frac{1}{2}}}{\zeta^{\frac{1}{2}}+\bar{\rho}^{\frac{1}{2}}} + \frac{Q}{\pi k^*} \arg(\rho^{\frac{1}{2}}) + iH\,. \tag{5.3}$$

Substitution of:

$$\zeta = \lambda\, e^{i\theta} \tag{5.4}$$

and

$$\rho = e^{i\alpha} \tag{5.5}$$

in eq. (5.3) and subsequent separation of real and imaginary part yields:

$$x = -\frac{H}{\pi} \ln \lambda - \frac{Q}{\pi k^*} \arctan\left\{\frac{2 \sin \frac{1}{2}\alpha\,[\lambda^{\frac{1}{2}} \cos \frac{1}{2}\theta + \cos \frac{1}{2}\alpha]}{\lambda + 2\lambda^{\frac{1}{2}} \cos \frac{1}{2}\theta \cos \frac{1}{2}\alpha + \cos \alpha}\right\} + \frac{Q}{\pi k^*} \tfrac{1}{2}\alpha \tag{5.6}$$

$$y = H \frac{\pi-\theta}{\pi} + \frac{Q}{2\pi k^*} \ln\left\{\frac{\lambda + 2\lambda^{\frac{1}{2}} \cos \frac{1}{2}(\theta-\alpha)+1}{\lambda + 2\lambda^{\frac{1}{2}} \cos \frac{1}{2}(\theta+\alpha)+1}\right\}. \tag{5.7}$$

The position of the drain in z $(z_R = x_R + iy_R)$ is found from eqs. (5.6) and (5.7) by putting $\lambda\, e^{i\theta} = e^{i\alpha}$. This gives:

$$x_R = 0$$

$$y_R = H \frac{\pi-\alpha}{\pi} - \frac{Q}{\pi k^*} \ln(\cos \tfrac{1}{2}\alpha)\,. \tag{5.8}$$

The latter equation becomes after division by H and denoting the distance of the drain above the x-axis (y_R) by h_0:

$$\frac{h_0}{H} = \frac{\pi-\alpha}{\pi} - \frac{Q}{\pi k^* H} \ln(\cos \tfrac{1}{2}\alpha)\,. \tag{5.9}$$

The equation for the interface can be found from eqs. (5.6) and (5.7) by putting $\theta = \pi$. (the interface is mapped onto the negative ξ-axis.) One finds the height of S (see Fig. 11) above the x-axis by putting $\theta = \pi$ and $\lambda = 1$ in eq. (5.7). This gives:

$$\frac{h}{H} = \frac{Q}{\pi k^* H} \ln\left[\text{cotan}\, \tfrac{1}{4}(\pi-\alpha)\right]. \tag{5.10}$$

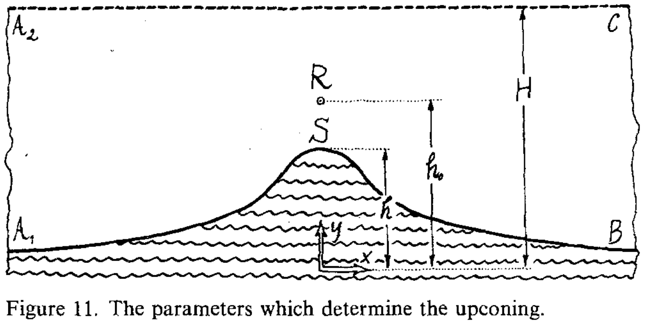

Figure 11. The parameters which determine the upconing.

Elimination of α from eqs. (5.9) and (5.10) finally yields:

$$\frac{h_0}{H} = \frac{4}{\pi} \arctan\left\{\exp\left(-\frac{\pi k^* h}{Q}\right)\right\} + \frac{Q}{\pi k^* H} \ln\left(\cosh \frac{\pi k^* H}{Q}\right) \tag{5.11}$$

Equation (5.11) is represented graphically in Fig. 12.

Instability of the interface occurs if the top of the cone becomes a cusp (cf. Fig. 9b). Then, the mapping of ζ onto z is not longer conformal in point S and therefore the derivative of z with respect to ζ vanishes there:

$$\left(\frac{dz}{d\zeta}\right)_{\zeta=-1} = 0 .$$

From this, one finds by use of eqs. (5.3) and (5.5) that a cusp originates if

$$\frac{Q}{\pi k^* H} = 2 \operatorname{cotan}(\tfrac{1}{2}\alpha) . \tag{5.12}$$

Elimination of α from eqs. (5.10) and (5.12) gives:

$$\frac{h}{H} = \frac{Q}{\pi k^* H} \operatorname{arcsinh}\left(\frac{2}{\pi}\cdot\frac{\pi k^* H}{Q}\right) . \tag{5.13}$$

Eq. (5.13) bounds the graph in Fig. 12 on the upper right.

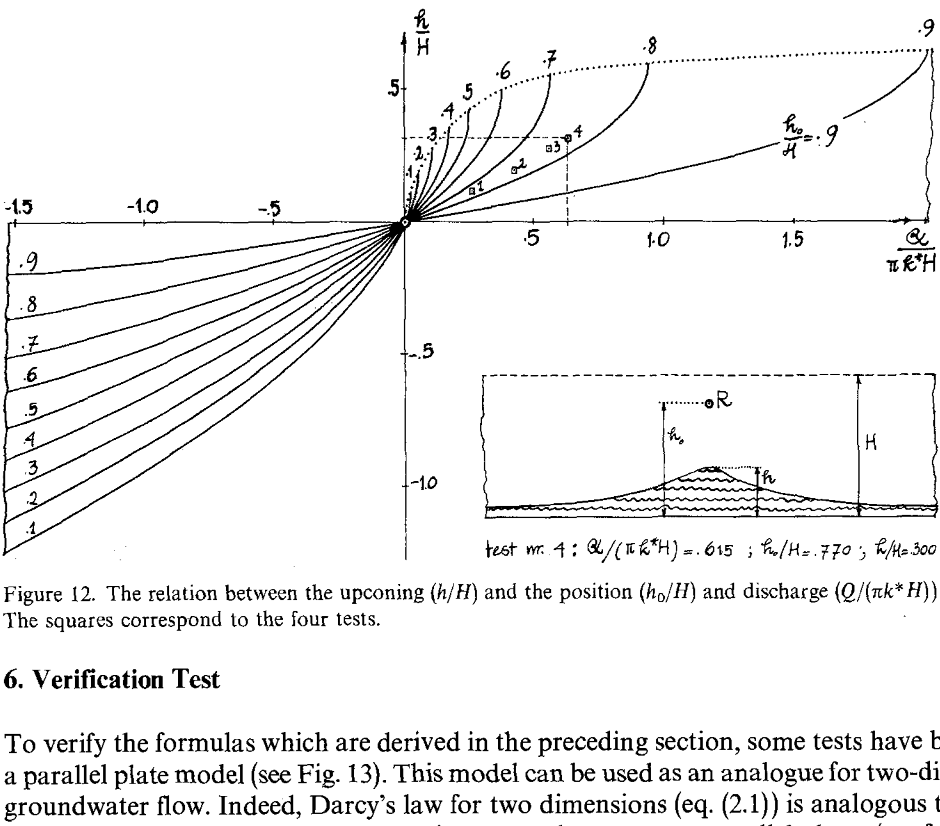

Figure 12. The relation between the upconing (h/H) and the position (h_0/H) and discharge ($Q/(\pi k^* H)$) of the drain. The squares correspond to the four tests.

6. Verification Test

To verify the formulas which are derived in the preceding section, some tests have been run in a parallel plate model (see Fig. 13). This model can be used as an analogue for two-dimensional groundwater flow. Indeed, Darcy's law for two dimensions (eq. (2.1)) is analogous to the flow of a viscous fluid through the narrow interspace between two parallel plates (see for instance [5]). The value of k^* can be found from the following equation:

$$k^* = [(\gamma_s - \gamma_f)/\gamma_f]\, g d^2/(12\nu)$$

where γ_s and γ_f are the specific weights of the heavier and the lighter fluid respectively, g is the acceleration of gravity, d is the distance between the parallel plates and ν is the dynamic viscosity of the lighter fluid. The distance between the parallel plates was not completely constant over the model, but varied between 1.85 and 2.00 mm. An average value for d has been computed in the following way, suggested by mr. A. Mensinga, who run the tests. The model has been completely filled with a known volume of water (V). The area (A) of the model is known, and d could be computed from:

$$d = \frac{V}{A} \approx 1.93 \text{ mm} .$$

The other constants in eq. (6.1) had the following values:

$$\begin{aligned} \gamma_s &= 1.00305 \text{ gf/cm}^2 \\ \gamma_f &= 0.8686 \text{ gf/cm}^2 \\ g &\approx 981 \text{ cm/sec}^2 \\ \nu &= 0.325 \text{ cm}^2\text{/sec} \quad \text{for a temperature of } 22.2°\text{C} . \end{aligned}$$

Substitution of these values in eq. (6.1) gives:

$$k^* = 1.46 \text{ cm/sec} . \tag{6.2}$$

Four tests have been run, all of them with one drain in the fresh water region. The position of each test is denoted by a square in the graph of Fig. 12. A photograph of the test with the largest discharge of the drain is presented in Fig. 13. The streamlines are visualized by injecting from

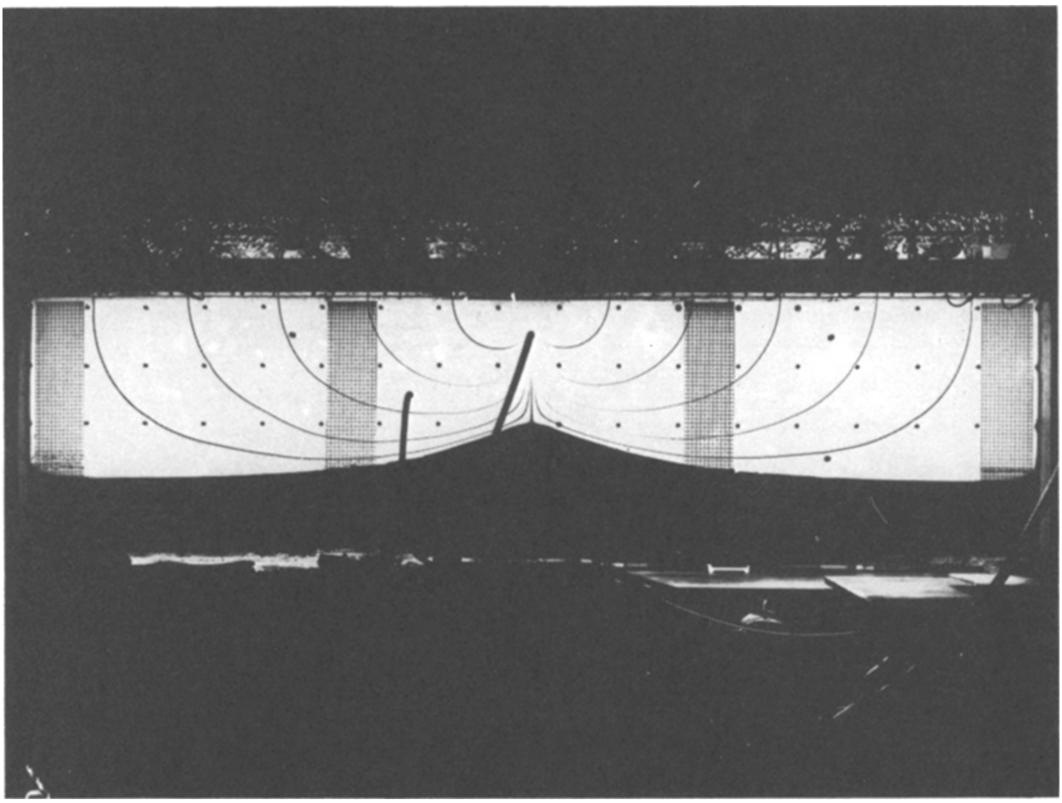

Figure 13. The photograph of test nr. 4.

above a red colored fluid of the same specific weight and viscosity as the lighter fluid. It must be noted, that the actual interface is a little lower than is seen on the photograph. This is caused by the injection of the red colored fluid on both ends of the upper boundary of the model, which was necessary in order to visualize the stagnation point S and the streamline connecting it with the drain (see Fig. 13).

The values of Q (the discharge of the drain), h_0, H and h (see Fig. 11) were measured during the four tests:

Test number	1	2	3	4	
Q (cm^2/sec)	54.3	85.9	114.5	128.9	
h_0 (cm)	33.3	34.1	34.9	35.2	(6.3)
H (cm)	43.8	44.6	45.4	45.7	
h (cm)	5.0	8.4	12.0	13.7	(6.4)

The dimensionless parameters $Q/(\pi k^* H)$, h_0/H and h/H, as used in the preceding section are found from eqs. (6.3), (6.4) and (6.2):

Test number	1	2	3	4	
$Q/(\pi k^* H)$	0.270	0.420	0.550	0.615	(6.5)
h_0/H	0.760	0.765	0.769	0.770	
h/H	0.114	0.188	0.264	0.300	(6.6)

In order to compare the test results with the theory, the upconing (h/H) will be computed from eqs. (5.9) and (5.10) by use of eq. (6.5). To that end, first the value of α is computed from eq. (5.9):

$$\frac{h_0}{H} = \frac{\pi - \alpha}{\pi} - \frac{Q}{\pi k^* H} \ln\left[\cos\left(\tfrac{1}{2}\alpha\right)\right] \tag{6.7}$$

which gave for the four tests:

Test number	1	2	3	4	
α	47.50°	49.62°	52.26°	54.36°	(6.8)

Now, by use of eqs. (5.10), (6.5) and (6.8) h/H can be found:

Test number	1	2	3	4
h/H	0.115	0.188	0.260	0.304

which is in good agreement with the values which are found from the four tests:

Test number	1	2	3	4
h/H	0.114	0.188	0.264	0.300

(cf. eq. (6.6)).

Finally, the equation for the interface has been found by insertion of the values for α, $Q/(\pi k^* H)$ and h_0/H from the tests in eqs. (5.6) and (5.7) wherein $\theta = \pi$, because the interface is mapped onto the negative ξ-axis. The interface which is computed in this way can hardly be distincted from the actual interface, as found in each test. Therefore, no separate figures with the interfaces computed from the theory are presented.

Appendix

Polygons with Internal Branch Points and Poles

The conformal mapping of a region inside a closed polygon onto the upper half plane im $\zeta \geqq 0$ ($\zeta = \xi + i\eta$) can be found by use of the Schwarz–Christoffel Integral:

$$w = \alpha \int_{\zeta_0}^{\zeta} \prod_{\nu=1}^{n} (\lambda - \zeta_\nu)^{-k_\nu} d\lambda + \beta \tag{A.1}$$

where n is the number of the corner points w_ν which are mapped onto $\zeta = \zeta_\nu$ ($\nu = 1, 2, \ldots, n$) and where the internal angles of the polygon are $\varphi_\nu = (1 - k_\nu)\pi$.

The integral (A.1) is also valid if the polygon overlaps [4], provided that the branch points are located on the boundary. This property is used for the first time in groundwater flow by De Josselin de Jong [2].

A modification of the Schwarz–Christoffel Integral will be discussed which accounts for internal branch points (for the values of ζ, given by $\zeta = \gamma_i$; $i = 1, 2, \ldots, m$) and for poles in the interior region of the polygon (for the values of ζ, given by $\zeta = \rho_j$; $j = 1, 2, \ldots, l$) (see Fig. 14).

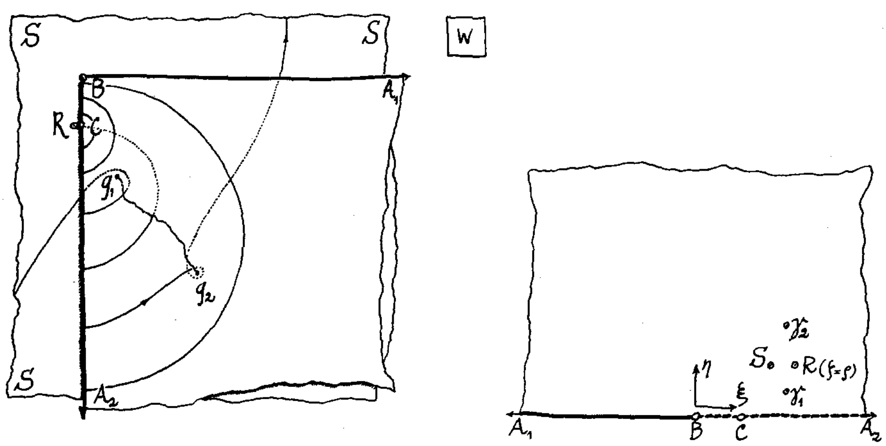

Fig. 14. The w-plane consists of two sheets. The branch points (2) are internal. There is one pole in the interior region (S). (cf. also Fig. 6c).

To start with, the following expression is considered:

$$w = \alpha \int_{\zeta_0}^{\zeta} \prod_{\nu=1}^{n} (\lambda - \zeta_\nu)^{-k_\nu} \prod_{i=1}^{m} (\lambda - \gamma_i)(\lambda - \bar{\gamma}_i) \prod_{j=1}^{l} [(\lambda - \rho_j)(\lambda - \bar{\rho}_j)]^{-2} h(\lambda) d\lambda + \beta \tag{A.2}$$

where γ_i ($i = 1, 2, \ldots, m$) and ρ_j ($j = 1, 2, \ldots, l$) are constants and where $h(\zeta)$ represents a function which will be determined later. The function $w(\zeta)$, presented in eq. (A.2), has poles of the first order for $\zeta = \rho_j$ and $\zeta = \bar{\rho}_j$ as well as internal branch points of the first order for $\zeta = \gamma_i$ and $\zeta = \bar{\gamma}_i$. Branch points of higher order are formed if some of the γ_i coincide. The integrand of eq. (A.2) is symmetric with respect to the ξ-axis, if the function $h(\zeta)$ fulfills the following condition:

$$\operatorname{Im}(h(\xi)) = 0\,. \tag{A.3}$$

Then, the integrand has the property that its argument is constant between two consecutive corner points. This is the well known property of any Schwarz–Christoffel Integral.

In order that the mapping is conformal in the poles, the condition:

$$\operatorname*{Res}_{\zeta = \rho_j} (dw/d\zeta) = 0 \tag{A.4}$$

must be fulfilled, (cf. [4]) as can be concluded from the Laurent expansion of $w(\zeta)$ around ρ_j.

For $m=0$ and $l=1$, eq. (A.2) together with eq. (A.4) reduces to the well known Schwarz–Christoffel Integral, which maps the exterior of a polygon onto the upper half plane (cf. [4]). From the conformality of the mapping (except in the points γ_i and ξ_ν) and from eq. (A.3) it follows, that $h(\zeta)$ is an analytic function for all ζ in im $\zeta \geqq 0$. By means of Schwarz's Reflection Principle, $h(\zeta)$ can be continued analytically into im $\zeta < 0$, from which it is deduced, that $h(\zeta)$ is analytic for all ζ. Hence, $h(\zeta)$ can be determined from its behaviour near infinity by use of Liouville's Theorem. If, for brevity's sake, the case is considered that a regular point of the boundary is transformed to infinity, the Laurent expansion of $w(\zeta)$ near infinity is:

$$w(\zeta) = w(\infty) + \alpha_1 \zeta^{-1} + \alpha_2 \zeta^{-2} + \ldots$$

Hence:

$$dw(\zeta)/d\zeta = -\alpha_1 \zeta^{-2} + O(\zeta^{-3}) . \tag{A.5}$$

The form near infinity of the function $w(\zeta)$ as given in eq. (A.2) is:

$$dw/d\zeta = \alpha \zeta^{-\sum_{\nu=1}^{n} k_\nu + 2m - 4l} h(\zeta) \qquad (\zeta \to \infty) .$$

Comparison with the Laurent expansion for $w(\zeta)$, which is given in eq. (A.5), shows that the following unequality holds near infinity:

$$h(\zeta) \leqq |M| \, |\zeta|^{\sum_{\nu=1}^{n} k_\nu + 4l - 2m - 2}$$

provided that $|M|$ is chosen large enough.

Since $h(\zeta)$ is analytic for all ζ, it can be deduced from Liouville's Theorem that $h(\zeta)$ is a polynomial of the order:

$$\sum_{\nu=1}^{n} k_\nu + 4l - 2m - 2 . \tag{A.6}$$

However, $h(\zeta)$ possesses no zeros since such would indicate additional branch points for $w(\zeta)$. Therefore, the order of the polynomial must be zero and $h(\zeta)$ reduces to a constant and, by appropriate choice of α, (see eq. (A.2)) to unity:

$$h(\zeta) = 1 \tag{A.7}$$

so that the condition (A.3) is fulfilled. Furthermore, the order of the polynomial is given by eq. (A.6) and vanishes only if:

$$\sum_{\nu=1}^{n} k_\nu + 4l - 2m - 2 = 0$$

or:

$$m = \frac{1}{2} \sum_{\nu=1}^{n} k_\nu + 2l - 1 \tag{A.8}$$

where the number $\Sigma_{\nu=1}^{n} k_\nu$ is even, since a regular point of the boundary is transformed to infinity and since the polygon is closed. Hence:

$$\sum_{\nu=1}^{n} k_\nu \pi = N \cdot 2\pi$$

where N equals the number of sheets in the w-plane, disregarding the poles. The final form of $w(\zeta)$ can be derived from eqs. (A.4) and (A.7). This yields:

$$w = \alpha \int_{\zeta_0}^{\zeta} \prod_{\nu=1}^{n} (\lambda - \xi_\nu)^{-k_\nu} \prod_{i=1}^{m} (\lambda - \gamma_i)(\lambda - \bar{\gamma}_i) \prod_{j=1}^{l} [(\lambda - \rho_j)(\lambda - \bar{\rho}_j)]^{-2} \, d\lambda + \beta \tag{A.9}$$

where the number m can be found from eq. (A.8) if the sum of the values for k_ν $(\Sigma_{\nu=1}^{n} k_\nu)$, as well as the number of the poles (l) is known.

In case a corner point of the polygon is transformed to infinity, the corresponding term must bé left out from eq. (A.9) but not the corresponding value for k_v from eq. (A.8).

A special case of the function, presented in eq. (A.9) is derived by Koppenfels and Stallmann (see [4], pp. 151–154) being the solution of a torsion problem. They did, however, not relate the solution to the geometrical properties of the polygon.

Acknowledgements

I am grateful to Professor Dr. Ir. G. de Josselin de Jong, because he stimulated me to write this paper. I highly appreciate the remarks of Dr. Ir. A. Verruijt. I am indebted to Dr. Ir. J. W. Reijn for his many useful and necessary remarks regarding the presentation of this study and the form of this paper.

REFERENCES

[1] J. Bear and G. Dagan, *Intercepting fresh water above the interface in a coastal aquifer*, General Assembly of Berkely, Commission of Subterranian Waters, IASH, publ. nr. 64, Gentbrugge (1964).
[2] G. de Josselin de Jong, A many valued hodograph in an interface problem, *Water Resources Research*, 1, 4 (1965) 543–555.
[3] A. Verruijt, An interface problem with a source and a sink in the heavy fluid, *Journal of Hydrology*, 8 (1969) 197–206. North Holland Publishing Co., Amsterdam.
[4] W. von Koppenfels and F. Stallmann, *Praxis der Konformen Abbildung*, Springer Berlin, Bd. 100 (1959).
[5] A. Verruijt, *Theory of groundwater flow*, MacMillan, London (1970).
[6] M. Muskat, *The flow of homogeneous fluids through porous media*, McGraw-Hill, Ann Arbor (1937).
[7] P. Ya. Polubarinova-Kochina, *Theory of groundwater movement*, Princeton University Press, Princeton (1962).